Kinetic Study of Enzymatic Urea Hydrolysis in the pH Range 4–9

M. Fidaleo and R. Lavecchia*
Dipartimento di Scienze e Tecnologie Agroalimentari,
Università della Tuscia, Via S. Camillo de Lellis, I-01100 Viterbo (Italy)
*Dipartimento di Ingegneria Chimica, Università "La Sapienza",
Via Eudossiana 18, I-00184 Roma (Italy)

Professional paper
Received: Juny 16, 2003
Accepted: September 1, 2003

The enzymatic hydrolysis of urea by jack bean urease was investigated at 25 °C over the pH range 4–9. Reaction rate data were found to be well described by a modified Michaelis-Menten equation with a pH-dependent rate coefficient and a product inhibition term. The influence of pH on activity was interpreted in terms of perturbation of the enzyme distribution among three differently protonated forms. Kinetic analysis yielded a Michaelis constant of 3.21 mmol l^{-1} and indicated that the inhibition mechanism was of the fully non-competitive type, with K_P = 12.2 mmol l^{-1}. The estimated activation energy was 35.3 kJ mol^{-1}. The resulting kinetic expression was tested by comparing model predictions with the experimental behaviour observed in unbuffered media and over a long-term period.

Keywords:
Enzyme kinetics, urease, urea, hydrolysis

Introduction

Urease is a nickel-containing enzyme that catalyses the hydrolysis of urea into ammonia and carbon dioxide.[1] This enzyme occurs in such different organisms as bacteria, algae, fungi and higher plants. Its primary function is allowing the organism to use urea as a nitrogen source. In plants, urease is involved in systemic nitrogen transport pathways, and is thought to act as a toxic defence protein.[2] In humans, bacterial ureases are important virulence factors in a number of diseases of the urinary tract and gastroduodenal region, including cancer.[3]

The increasing need for specifically removing urea from far different environments has prompted a growing biotechnological interest in this enzyme.[4] Actual or potential applications range from the treatment of industrial wastes[5,6] or alcoholic beverages[7] to the design of life-support systems for manned space missions.[8] Systems based on immobilised or microencapsulated urease are also being studied for use in haemodialysis.[9,10]

For the optimal design and analysis of all of the above devices an accurate knowledge of the enzyme kinetics is required. As revealed by the number of published papers, the catalytic properties of urease have been thoroughly investigated, and many aspects of the molecular mechanisms of action have been elucidated.[4,11–13] What is lacking, by contrast, is the availability of simple but reliable kinetic expressions for the dependence of the hydrolysis rate on the solution properties and, particularly, on pH.

The influence of pH on activity is usually described in terms of perturbations of the enzyme distribution among differently protonated forms.[14] Mathematical treatment of the mechanism considered yields the dependence of the apparent kinetic quantities, such as the Michaelis constant, K_M, and the maximum reaction rate, v_{max}, on pH.

Barth and *Michel*[15] analysed the activity of the 12 S unit of urease in the pH range 4–9, and found a sharp dependence of both K_M and v_{max} on pH. In particular, K_M displayed a minimum at pH 7, whereas v_{max} was maximal at the same pH. *Krajewska* and *Zaborska*[16] investigated the effects of phosphate buffer on the kinetic behaviour of free urease in the pH range 5.8–8.1. Their results indicated that this buffer can act as a competitive enzyme inhibitor. Furthermore, while the maximum reaction rate exhibited the classic bell-shaped pH dependence, the Michaelis constant extrapolated to zero buffer concentration was only moderately affected by pH. In another study performed in buffer-free solutions, K_M was found to be practically independent on pH, and pH effects on v_{max} were described by an empirical equation containing five parameters.[17] Still different results were obtained for immobilized[18–20] or gel-entrapped[21] urease. For these systems, however, the presence of perturbations resulting from partitioning effects and diffusional limitations should be taken into consideration.

*Corresponding author

In addition to the above points, determination of adequate kinetic expressions is greatly complicated by the peculiar features of the urea-urease system. In aqueous solution the reaction products, ammonia and carbon dioxide, can exist in different ionic states, each affecting the reaction rate.[22] Moreover, urease is subject to, both, substrate and product inhibition. Responsible for the latter is the ammonium ion, which inhibits the enzyme by a non-competitive mechanism.[17–23] Results of long-term experiments indicated that this species can also act as an irreversible poison to urease.[24] Finally, urea is a powerful protein denaturant, only slightly less denaturing than guanidine hydrochloride.[25] As a result, a particular care should be paid to planning experiments and estimating kinetic parameters from reaction rate data.

The aim of this study was to derive a simple kinetic expression for the enzymatic hydrolysis of urea over an extended pH range and under controlled reaction conditions. We were also interested in assessing whether the kinetic quantities so obtained, although determined from macroscopic measurements, could be related to some aspect of the enzymatic mechanism of action. Attention was focused on urease from jack bean seeds, the main commercial source of the enzyme, and experiments were carried out in buffered and unbuffered media.

Experimental procedure

Materials

Urease (EC 3.5.1.5) from *Canavalia ensiformis* (jack bean) seeds was obtained from Sigma Chemical Co. (St. Louis, MO) as a lyophilised and chromatographically purified powder. The claimed activity was 22 U mg^{-1}, where 1 U corresponds to the amount of enzyme that liberates 1 μmol of NH_3 from urea per minute at 25 °C and pH 7. The free ammonia was < 0.05 μg per unit. Urea and ammonium carbamate were purchased from Carlo Erba (Milano, Italy) with purities greater than 99.5 %.

Ammonium carbonate solutions were prepared by dissolving known amounts of ammonium carbamate into bidistilled water. Enzyme solutions in water or buffer were prepared just before use. The buffers used were: acetate (0.1 mol l^{-1}, pH 4 and 5), phosphate (0.1 mol l^{-1}, pH 6 and 7) and borate (0.1 mol l^{-1}, pH 8 and 9). All chemicals were of reagent grade and used without further purification.

Methods

Kinetic runs were performed in magnetically stirred 50 ml flasks immersed in a circulating water bath. The temperature was controlled within ± 0.1 °C by an external thermostat equipped with a digital temperature programmer (Haake, PG 41). In a typical experiment, about 30 ml of the urea containing solution were poured into the flask and thermostated, under agitation, for at least 20 min. Reaction was started by adding 5 ml of the enzyme solution. At selected times, aliquots were withdrawn, and analysed for ammonium content by a reagent kit (Spectroquant® Ammonium, Merck) based on the indophenol blue method. Optical measurements were made at 690 nm by a double-beam UV-VIS spectrophotometer (Perkin Elmer, Lambda 5).

Runs aimed at investigating product inhibition were carried out by adding known amounts of ammonium carbonate to the reaction medium. Substitution of ammonium carbonate with ammonium chloride did not produce any significant change in the results obtained.

The pH of the reacting system was continuously monitored. In the absence of buffers, the solution reached almost instantaneously a value close to 9.4.

Plan of experiments

Several sets of experiments were performed, under the conditions summarised in Table 1. The first set of runs (series *A*) was made to analyse the effects of urease concentration. To investigate the influence of pH six sets of experiments (series *B–G*) were carried out. In these runs the temperature was maintained at 25 °C and the pH was varied between 4 and 9. A further set of runs was performed at 37 °C and pH 7 to estimate the activation energy of reaction (series *H*). Product inhibition was studied at 25 °C and pH 7, by adding different amounts of ammonium to the reaction medium (series *I–J*). Finally, four sets of experiments were conducted to validate the kinetic expression considered: in buffer-free systems (series *K–L*) and over a long-term period (series *M–N*).

Results and discussion

Analysis of kinetic data

The enzymatic hydrolysis of urea can be represented by the overall reaction:[22]

$$(NH_2)_2CO + 2\ H_2O \rightarrow 2\ NH_4^+ + CO_3^{2-}$$

Assuming a non-competitive mechanism for ammonium inhibition[23] leads to the following rate expression:

$$r = \frac{v_{max} \cdot [S]}{(K_M + [S])\left(1 + \frac{[P]}{K_P}\right)} \quad (1)$$

where [S] and [P] are the substrate and ammonium ion concentrations, v_{max} is the maximum reaction rate, K_M is the Michaelis constant, and K_P is the dissociation constant for the enzyme-product complex.

Kinetic data were analysed by the initial-rate method, calculating reaction rates from the values of the slope of the concentration-time plots. Data points were taken over a time period of 0.5 to 2 min.

Parameter estimation was carried out by minimisation of the following objective function:

$$\Phi = \max_{i=1,n_D} \left| r_{i,exp} - r_{i,calc} \right| \tag{2}$$

where n_D is the number of data points and the subscripts *exp* and *calc* denote experimental and calculated quantities, respectively. Minimum search was performed by the Nelder-Mead simplex algorithm.[26] It is a direct-search method which does not require gradient calculations or derivative information. To find the global minimum the parameter space was explored by random generation of starting points.

Effect of urease concentration

Experiments made at 25 °C, pH 7 and constant urea concentration, showed that, up to 0.2 g l^{-1}, reaction rate is proportional to urease concentration (Figure 1). This result indicates that the specific enzyme activity remains constant, within the urease concentration range considered, and that protein denaturation does not occur.

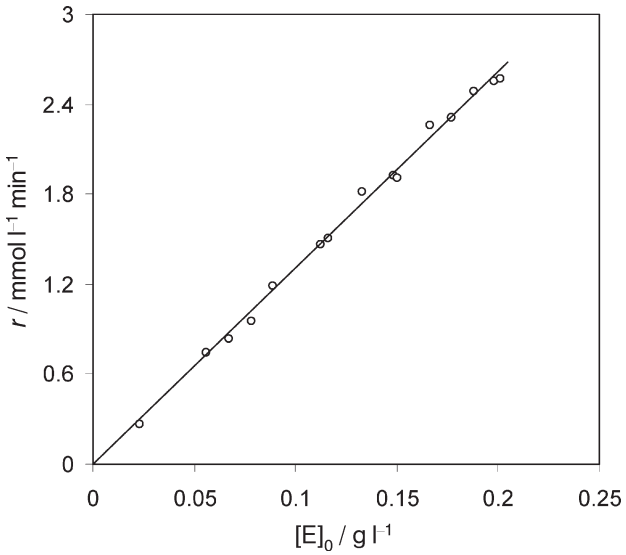

Fig. 1 – *Effect of urease concentration on the rate of urea hydrolysis at 25 °C and pH 7. Other experimental conditions are given in Table 1 (series A).*

Effect of pH

Since the kinetic data were analysed by the initial-rate method, the term $[P]/K_P$ in eqn. (1) was assumed to be much smaller than 1, so as to obtain:

$$r = \frac{v_{max} \cdot [S]}{K_M + [S]} \tag{3}$$

From a physical viewpoint interpreting rate data by the above equation means to say that, at short reaction times, product inhibition phenomena give a negligible contribution to the overall kinetics. To determine the pH dependence of v_{max} and K_M, we assumed the mechanism described by *Tripton* and *Dixon*,[14] which is illustrated in Figure 2. In this scheme $K_{E,1}$ and $K_{E,2}$ are the molecular dissociation constants for the free enzyme, and $K_{ES,1}$ and $K_{ES,2}$ are those for the enzyme-substrate complex.

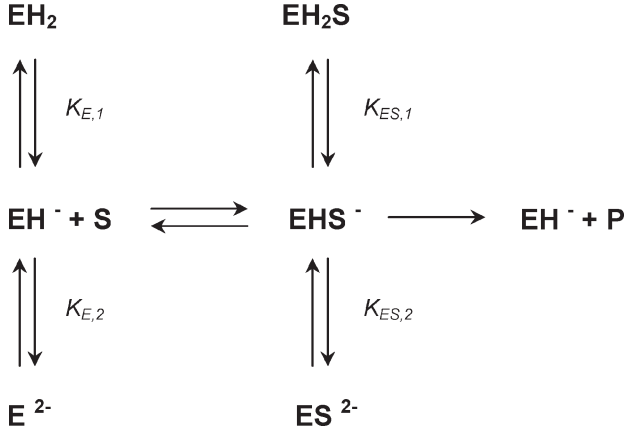

Fig. 2 – *Schematic diagram of the mechanism assumed to describe pH effects on the enzymatic urea hydrolysis (E, S and P represent the enzyme, substrate and product species, with the former distributed among three differently protonated forms)*

Steady-state treatment of the mechanism yields:

$$v_{max} = \frac{k \cdot [E]_0}{1 + \dfrac{[H^+]}{K_{ES,1}} + \dfrac{K_{ES,2}}{[H^+]}} \tag{4}$$

$$K_M = K_{M0} \frac{1 + \dfrac{[H^+]}{K_{E,1}} + \dfrac{K_{E,2}}{[H^+]}}{1 + \dfrac{[H^+]}{K_{ES,1}} + \dfrac{K_{ES,2}}{[H^+]}} \tag{5}$$

where k is the rate coefficient, $[E]_0$ is the total enzyme mass concentration and $[H^+]$ is the concentration of hydrogen ions.

We first estimated the quantities v_{max} and K_M at each pH, obtaining the results presented in Figure 3.

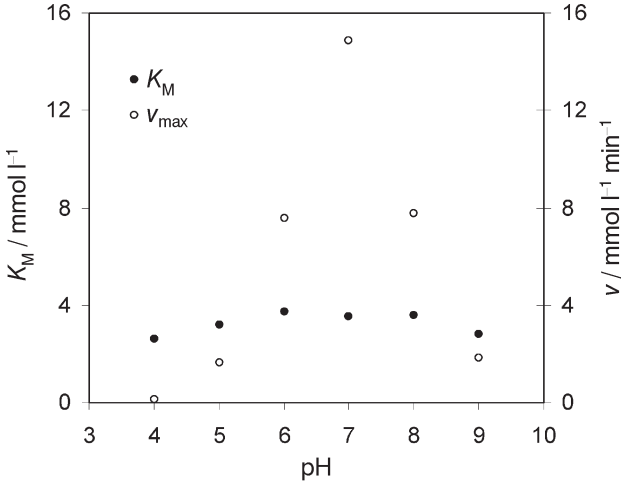

Fig. 3 – *Estimated v_{max} and K_M at 25 °C and various pH values. Other experimental conditions are given in Table 1 (series B–G)*

The plot indicates that pH effects on K_M are much smaller than those on v_{max}, at least over the pH range considered. Accordingly, the Michaelis constant was assumed to be pH independent ($K_M = K_{M0}$) and eqn. (3) was written as:

$$r = \frac{k \cdot [E]_0 \cdot [S]}{\left(1 + \frac{[H^+]}{K_{ES,1}} + \frac{K_{ES,2}}{[H^+]}\right)(K_M + [S])} \qquad (6)$$

This equation contains four variables: k, K_M, $K_{ES,1}$ and $K_{ES,2}$. They were determined by minimisation of the objective function defined by eqn. (2), obtaining the results reported in Table 2. Representative examples of experimental and calculated kinetic curves are shown in Figure 4. As apparent, the agreement is very good.

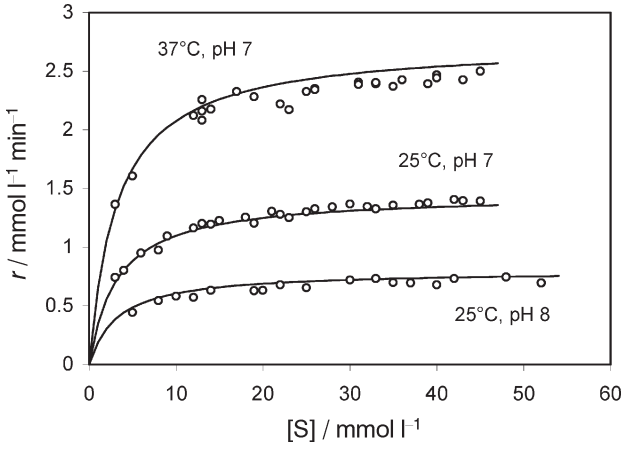

Fig. 4 – *Experimental and calculated hydrolysis rates at different pH and temperature conditions. Experimental conditions are given in Table 1 (series E, F and G). Solid curves are calculated from eqn. (6) using the quantities listed in Table 2.*

The Michaelis constant estimated by us falls within the range of values reported in the literature for this type of urease.[4,17] It should be noted, however, that most of published results were obtained in unbuffered media, or with buffers at neutral or near-neutral pH. Our results indicate that K_M can be taken as a constant over the pH range 4–9, and that it is not influenced by the nature of buffer components.

According to eqn. (5), constancy of K_M implies $K_{E,1} = K_{ES,1}$ and $K_{E,2} = K_{ES,2}$, *i.e.* that the ionisation constants are not affected by substrate binding. This suggests that the effect of hydrogen ions on activity is fully non-competitive. From the resulting dissociation constants the following pK values are obtained: pK_1 = 6.12 and pK_2 = 7.90. They correspond to an optimal pH of 7.01. As regards the molecular significance of the observed pK's it seems interesting to note that pK_1 is close to 6.5, the pK_a of free histidine, and that pK_2 could be reasonably ascribed to a metal-bound water.[12] If the observed pH dependence is interpreted in terms of the reverse protonation model,[27,28] the involvement of a protonated histidine residue and a deprotonated water, would then result.

The above view is consistent with the mechanism proposed by Karplus et al.[12] for *K. aerogenes* urease, according to which one of the two nickel ions in the active site of urease co-ordinates urea via its carbonyl oxygen, while the other binds and activates a hydrolytic water molecule (*Wat-502*). Their results also indicate that all four urea protons are hydrogen bonded to four active-site residues (*Ala167*, *Cys319*, *Gly277* and *Ala363*). This binding mode, along with considerations on the nature and position of the active-site residues, leads to a very efficient mechanism of reaction, where *Wat-502* attacks the carbonyl carbon of urea to form a hydrated urea intermediate, and *His320* protonates the urea nitrogen. Once the *N*-protonated intermediate is formed, ammonia is eliminated and the bound carbamate dissociates from the enzyme.

It seems interesting to point out that the reverse protonation model predicts an active enzyme fraction, at the optimal pH, equal to $10^{-\Delta pK}$, with ΔpK = pK_2 – pK_1. Substitution of the values calculated by us gives a ΔpK of 1.78 and an active enzyme fraction of 1.66 %. This means to say that at the optimal pH only one in $10^{1.78}$ enzyme molecules have the correct protonation state for urea hydrolysis. Such a small amount of active urease must, of course, be largely counterbalanced by the enhanced reactivity of the active species.[12]

Effect of temperature

The activation energy of hydrolysis was estimated from reaction rate data at 25 and 37 °C (series *E* and *H* in Table 1). We assumed that k was the

Table 1 – *Outline of the experimental conditions (n_D is the number of data points, $[E]_0$, [S] and [P] are the concentrations of urease, urea and ammonium, respectively)*

Data set	n_D	Reaction medium	pH	$\frac{T}{°C}$	$\frac{[E]_0}{g\ l^{-1}}$	$\frac{[S]}{mmol\ l^{-1}}$	$\frac{[P]}{mmol\ l^{-1}}$
A	15	Phosphate buffer	7	25	0.02–0.2	25	–
B	13	Acetate buffer	4	25	0.1	12–70	–
C	17	Acetate buffer	5	25	0.1	5–70	–
D	17	Phosphate buffer	6	25	0.1	5–45	–
E	26	Phosphate buffer	7	25	0.1	3–45	–
F	17	Borate buffer	8	25	0.1	5–52	–
G	16	Borate buffer	9	25	0.1	2–57	–
H	22	Phosphate buffer	7	37	0.1	3–39	–
I	11	Phosphate buffer	7	25	0.1	5	5–80
J	11	Phosphate buffer	7	25	0.1	30	5–80
K	29	Water	–	25	0.1	0.7–40	–
L	21	Water	–	37	0.1	8–55	–
M	8	Acetate buffer	5	25	0.1	20	–
N	8	Borate buffer	8	25	0.1	20	–

only temperature-dependent parameter in eqn. (6) and used the following expression:

$$k(T) = \exp\left[-\frac{E_a}{R}\left(\frac{1}{T} - \frac{1}{T^*}\right)\right] \qquad (7)$$

where E_a is the activation energy and T^* is the temperature at which k = 1 mol g^{-1} min^{-1}. Fitting eqn. (7) to the experimental data yielded: E_a = 35.3 kJ mol^{-1} and T^* = 414.6 K

The activation energy falls between the values of 32.6 kJ mol^{-1} and 35.8 kJ mol^{-1}, reported by *Huang* and *Chen*[29] and by *Martins* et al.[30] respectively. Such values were obtained in buffer, and are slightly higher than that (E_a = 29.1 kJ mol^{-1}) observed in buffer-free systems.[17]

Product inhibition

Product inhibition data were interpreted by considering a fully non-competitive inhibition mechanism. Fitting eqn. (1) to the experimental data, with the values of k, K_M, $K_{ES,1}$ and $K_{ES,2}$, determined previously, gave: K_P = 12.20 ± 1.09 mmol l^{-1}. Figure 5 shows the good agreement between experimental and calculated results. The fact that the data points, when plotted as *1/r* vs. [P], lie along a straight line, clearly supports the assumption of non-competitive product inhibition. The value of K_P found by us is lower than that obtained in buffer-free systems,[17] indicating that phosphate buffer increases urease sensitivity to inhibition by ammonium ions.

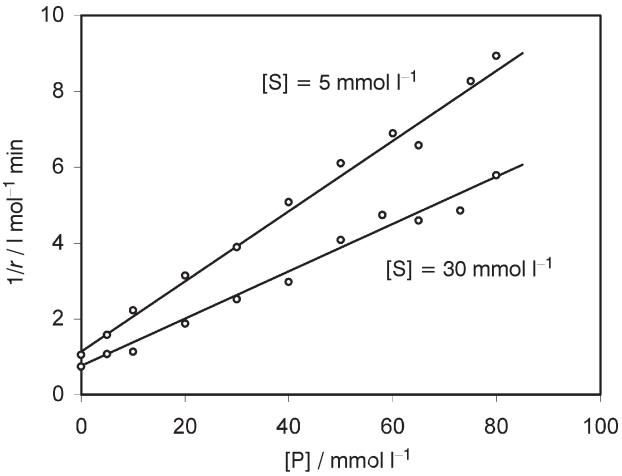

Fig. 5 – *Linearised plot showing the influence of ammonium concentration on the rate of urea hydrolysis at two different urea concentrations. Experimental conditions are given in Table 1 (series I and J). Straight lines are calculated from eqn. (1) using the quantities listed in Table 2.*

Statistical analysis of results

To assess the statistical significance of the results obtained we analysed the model residuals, defined as the difference between experimental and calculated reaction rates:

$$\rho_i = r_{i,exp} - r_{i,calc} \qquad (8)$$

In order to ensure that each data had the same statistical weight, residuals were normalised as:

$$\rho_i^* = \frac{\rho_i}{\left[\frac{1}{n_D - n_P}\sum_{i=1}^{n_D}\rho_i^2\right]^{0.5}} \quad (9)$$

where n_D is the number of data points and n_P is the number of model parameters. It can be shown[31] that, if the error is normally distributed, 95 % of the normalised residuals should be in the range ± 2. Calculation for data sets *B*–*G* (with n_D = 106 and n_P = 4) and *I*–*J* (with n_D = 22 and n_P = 1) gave the results displayed in Figure 6. As can be seen, residuals are uniformly scattered between –2 and +2, with just one outlier (ρ^* = 3.826). Moreover, no systematic concentration-related effect is observed. Similar considerations hold when plotting average residuals against pH (see inset in Figure 6).

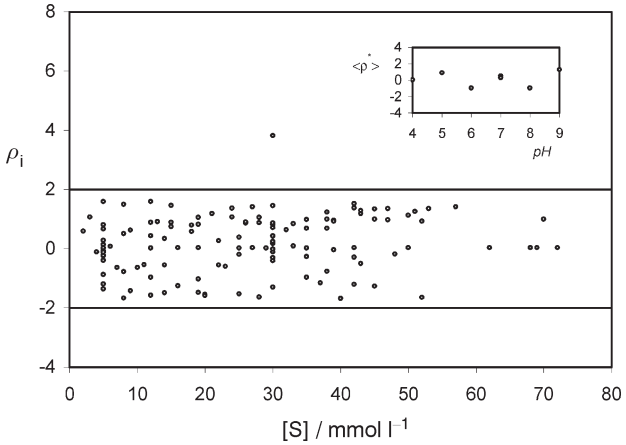

F i g . 6 – *Normalised model residuals as a function of substrate concentration. The horizontal lines at* $\rho_i^* = \pm 2$ *delimit the 95 % confidence region. The inset shows the trend of normalised average residuals,* $<\rho^*>$*, as a function of pH.*

As a further means of assessing the normality of the error distribution we made use of a normal probability plot. It is obtained by plotting the ordered residuals, ρ_i, against the corresponding normal order statistics medians, which are defined as

$$\mu_i = F^{-1}\left(\frac{i}{n_D + 1}\right) \quad (10)$$

where *F* is the standard normal cumulative distribution function. Data plotted in such a way should form an approximate straight line, with the intercept and slope representing, respectively, the location and scale parameters of the normal distribution.[32] By contrast, departures from linearity would be indicative of deviations from the assumed normal distribution. The diagram shown in Figure 7 illustrates the results obtained. As apparent, a highly linear pattern is observed (R^2 = 0.945), with just limited deviations in the lower and upper extremes. From

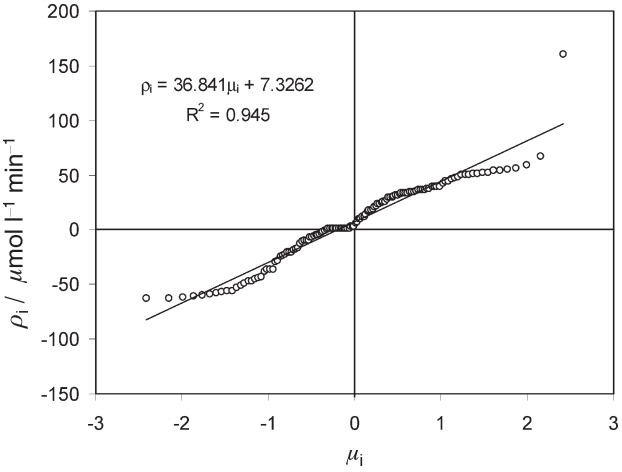

F i g . 7 – *Normal probability plot showing the trend of ordered residuals* (ρ_i) *against normal order statistics medians* (μ_i).

the resulting line equation, the following location and scale parameters are obtained: 7.33 10^{-6} and 36.8 · 10^{-6} mol l^{-1} min^{-1}.

Finally, the Kolmogorov-Smirnov test was performed. To this end we calculated the largest absolute difference (*D*) between the observed cumulative frequencies and those corresponding to the normal distribution. We obtained: *D* = 0.07. For our sample size (n_D = 128) the critical *D*-value[33] at the 0.05 significance level is D_c = 0.12. Since $D < D_c$ assumption that the data belong to a population with a normal distribution cannot be rejected, *i.e.*, the interpretation of reaction rate data by the model developed can be considered statistically correct.

Model validation

To sum up, the kinetic analysis of urea hydrolysis by jack bean urease provides the following rate law:

$$r = \frac{\exp\left[-\frac{E_a}{R}\left(\frac{1}{T} - \frac{1}{T^*}\right)\right]\cdot[E]_0\cdot[S]}{(K_M + [S])\left(1 + \frac{[P]}{K_P}\right)\left(1 + \frac{10^{-pH}}{K_{E,1}} + \frac{K_{E,2}}{10^{-pH}}\right)} \quad (11)$$

The values of the corresponding quantities are summarised in Table 2. These quantities were determined from experiments in buffer, analysing the reaction course at very short times. To evaluate the predictive capabilities of the kinetic expression so obtained we compared calculations by eqn. (11) with the results of runs performed at conditions different from those used for parameter estimation. In particular, we analysed initial-rate data in unbuffered media (series *K* and *L* in Table 1) and the time course (up to 1 hour) of ammonium formation at pH 5 and 8 (series *M* and *N*).

Table 2 – *Estimated kinetic quantities (mean value and 95 % confidence interval) for urea hydrolysis*

Quantities	Value	Units
k	(1.83 ± 0.05) 10^{-2}	mol g^{-1} min^{-1}
K_M	(3.21 ± 0.36) 10^{-3}	mol l^{-1}
$K_{ES,1}$	(7.57 ± 0.41) 10^{-7}	mol l^{-1}
$K_{ES,2}$	(1.27 ± 0.08) 10^{-8}	mol l^{-1}
K_P	(1.22 ± 0.11) 10^{-2}	mol l^{-1}

Figure 8 shows experimental data points into buffer-free systems at 25 and 37 °C, along with the corresponding predictions. The two curves were calculated by setting pH 9.4, *i.e.* the pH measured in the absence of buffers, in eqn. (11), and assigning to the various parameters the values determined in buffer. As can be seen, data points are more scattered than in buffer, but the model accurately reproduces the experimental trends.

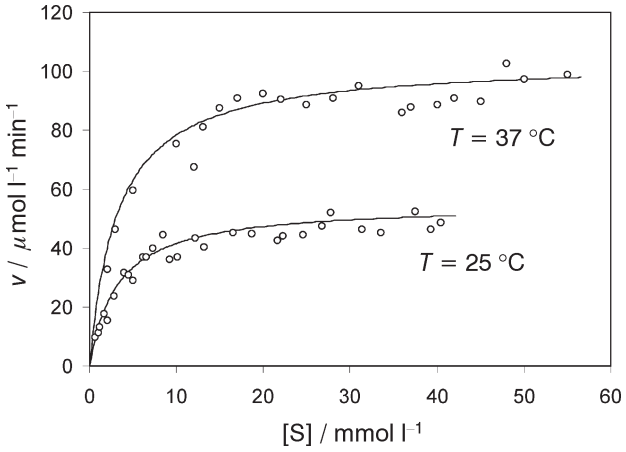

Fig. 8 – *Comparison between experimental initial-rate data in unbuffered media and model predictions. Experimental conditions are given in Table 1 (series K and L). Solid curves are calculated from eqn. (11) setting pH 9.4, [P] = 0 and using the quantities listed in Table 2.*

The results of long-term experiments (up to 1 hour) are presented in Figure 9. To model the time course of urea hydrolysis the unsteady mass-balance equations for the substrate and the product must be solved. Under the hypothesis of constant reactor volume, and accounting for the stoichiometric relationship: $r_P = 2\ (-r_S)$, the two equations can be written as:

$$-\frac{d[S]}{dt} = r([S],[P],[E]_0,T,pH) \qquad (12)$$

$$\frac{d[P]}{dt} = 2r([S],[P],[E]_0,T,pH) \qquad (13)$$

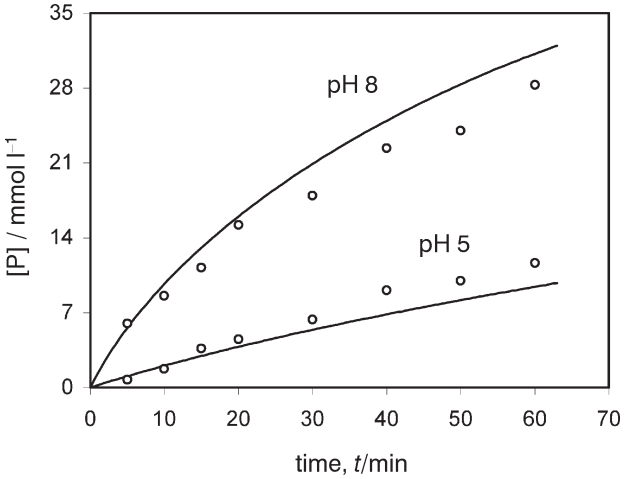

Fig. 9 – *Experimental and predicted time course of urea hydrolysis at 25 °C and two different pH. Experimental conditions are given in Table 1 (series M and N). Solid curves are calculated from eqns. (11)-(13) using the quantities listed in Table 2.*

and the initial conditions are: $[S]_{t=0}$ = 20 mmol l^{-1} and $[P]_{t=0}$ = 0.

The above set of ordinary differential equations was numerically solved, after substitution of the parameters listed in Table 2, by a fourth-order Runge-Kutta method. An examination of Figure 9 reveals that the kinetics of product formation at pH 5 and 8 is fairly well described, particularly within the first 20 min. At higher times product-formation rates are slightly overestimated (at pH 8), or underestimated (at pH 5). This could be due to the limited buffering capacity of the two buffers which, by a certain time, could lead to a pH increase due to the appearance and accumulation of ammonium and carbonate ions. In the solution with an initial pH of 5 the active enzyme fraction would then increase, with respect to its initial value. By contrast, in the solution with an initial pH of 8 the active enzyme fraction would be reduced. This effect could, of course, be accounted for by a more elaborated model considering the mass-balance equations for all the reacting species, the acid-base equilibria of buffer components, and the relations expressing the distribution of gaseous species between the liquid and the gas phases.

Conclusions

The experimental investigation carried out on jack bean urease allowed derivation of a simple kinetic expression for urea hydrolysis in the pH range 4–9. The parameters appearing in the resulting rate law were determined by the accurate initial-rate method. It was shown that a modified Michaelis-Menten equation, including a pH-dependent rate constant and a non-competitive product-inhibition term, well

describes the enzyme kinetics. Analysis of pH effects on activity indicated that the molecular dissociation constants for the free enzyme are not affected by substrate binding, provided that the enzyme is distributed among the three differently protonated forms considered. The corresponding p*K*'s are consistent with the molecular mechanism of action proposed for *K. aerogenes* urease, in which a protonated histidine and a deprotonated water are involved.

The good agreement between model predictions and the results obtained in unbuffered media and over a long-term period appears to support the assumptions on which the kinetic analysis was based. This conclusion is also validated by the statistical significance of the results obtained.

List of symbols

D – D-value for the Kolmogorov-Smirnov test
D_c – critical D-value
$[E]_0$ – total enzyme concentration, g l^{-1}
E_a – activation energy, J mol^{-1}
$[H^+]$ – hydrogen ions concentration, mol l^{-1}
k – rate coefficient, mol g^{-1} min^{-1}
K_E – molecular dissociation constant for the free enzyme, mol l^{-1}
K_{ES} – molecular dissociation constant for the enzyme-substrate complex, mol l^{-1}
K_M – Michaelis constant, mol l^{-1}
K_P – molecular dissociation constant for the enzyme-product complex, mol l^{-1}
n_D – number of data points
n_P – number of parameters
[P] – product concentration, mol l^{-1}
r – reaction rate, mol l^{-1} min^{-1}
R – universal gas constant, J mol^{-1} K^{-1}
R – correlation coefficient
[S] – substrate concentration, mol l^{-1}
t – time, min
T – temperature, K
T^* – kinetic parameter, K
v_{max} – maximum reaction rate, mol l^{-1} min^{-1}

Greek symbols

μ – normal order statistics medians
ρ – residual, mol l^{-1} min^{-1}
Φ – objective function, mol^2 l^{-1} min^{-2}

Subscripts

calc – calculated
exp – experimental
i – generic point

References

1. *Varner J. E.*, Urease, in Boyer, P. B., Lardy, H., Myrback, K., Eds., The Enzymes, Academic Press, New York, 1976, pp 247–256.
2. *Polacco J. C., Holland M. A.*, Int. Rev. Cytol. **145** (1993) 65.
3. *Burne R. A., Chen Y. Y.*, Microbes Infect. **2** (2000) 533.
4. *Qin Y., Cabral J. M. S.*, Biocat. Biotrans. **20** (2002) 1.
5. *Xu H. D., Chen R. R., Yao G. R., Liu X. X., Li G. M., Huang Y. P.*, Water Treat. **2** (1987) 136.
6. *George S., Chellapandian M., Sivasankar B., Jayaraman K.*, Bioprocess Eng. **16** (1997) 83.
7. *Matsumoto K.*, Bioprocess Technol. **16** (1993) 255.
8. *Schussel L. J., Atwater J. E.*, Chemosphere **30** (1995) 985.
9. *Keunbok L., Boadi D. K., Neufeld R. J.*, Chem. Eng. Sci. **50** (1995) 2263.
10. *Roberts M.*, Nephrology **4** (1998) 275.
11. *Jabri E., Carr M. B., Hausinger P.P., Karplus P.A.*, Science **268** (1995) 988.
12. *Karplus P. A., Pearson M. A., Hausinger R. P.*, Acc. Chem. Res. **30** (1997) 330.
13. *Ciurli S., Benini S., Rypniewski W. R., Wilson K. S., Miletti S., Mangani S.*, Coord. Chem. Reviews **190** (1999) 3315.
14. *Tipton K. F., Dixon H. B. F.*, Methods Enzymol. **63** (1979) 183.
15. *Barth A., Michel H. J.*, Biochem. Physiol. Pflanz. **163** (1972) 103.
16. *Krajewska B., Zaborska W.*, J. Mol. Catal. B **6** (1999) 75.
17. *Qin Y., Cabral J. M. S.*, Appl. Biochem. Biotechnol. **49** (1994) 217.
18. *Iyengar L., Bajpai P., Rao A. V., Prabhakara S.*, Indian J. Biochem. **19** (1982) 130.
19. *Moynihan H. J., Lee C. K., Clark W., Wang N. H. L.*, Biotech. Bioeng. **34** (1989) 951.
20. *Huang T. C., Chen D. H.*, J. Chem. Eng. Jpn. **25** (1992) 458.
21. *Atkinson B., Rott J., Rousseau I.*, Biotech. Bioeng. **19** (1977) 1037.
22. *Andrews R. K., Blakeley R. L., Zerner B.*, Adv. Inorg. Biochem. **6** (1984) 245.
23. *Hoare J. P., Laidler K. J.*, J. Am. Chem. Soc. **72** (1950) 2487.
24. *Ramachandran K. B., Perlmutter D. D.*, Biotech. Bioeng. **18** (1976) 685.
25. *Wu J. W., Wang Z. X.*, Protein Sci. **8** (1999) 2090.
26. *Nelder J. A., Mead R. A.*, Computer J. **7** (1965) 308.
27. *Mock W. L., Aksamawati M.*, Biochem. J. **302** (1994) 57.
28. *Mock W. L., Stanford D. J.*, Biochemistry **35** (1996) 7369.
29. *Huang T. C., Chen D. H.*, J. Chem. Tech. Biotechnol. **52** (1991) 433.
30. *Martins M. B. F., Cruz M. E. M., Cabral J. M. S., Kennedy J. F.*, J. Chem. Tech. Biotechnol. **39** (1987) 201.
31. *Himmelblau H.*, Process Analysis by Statistical Methods, J. Wiley & Sons, New York, 1970.
32. *Chambers J., Cleveland W., Kleiner B., Tukey P.*, Graphical Methods for Data Analysis, Wadsworth, New York, 1983.
33. *Draper N., Smith H.*, Applied Regression Analysis, J. Wiley & Sons, New York, 1998.